DALTON
FULL PAPER

Ferrocenyl phosphine mobility, positional isomerism and NMR fluxionality in triangular palladium sulfide aggregates. Crystal and molecular structures of $[Pd_3Cl_2(\eta^2\text{-dppf})(\mu\text{-dppf})(\mu_3\text{-S})_2]$ and $[Pd_3Cl(\eta^2\text{-dppf})_2(PPh_3)(\mu_3\text{-S})_2]X$ [X = Cl or NO_3, dppf = $Fe(\eta^5\text{-}C_5H_4PPh_2)_2$]

Jeremy S. L. Yeo,[a] Guangming Li,[a] Wai-Hing Yip,[b] William Henderson,[c] Thomas C. W. Mak *[b] and T. S. Andy Hor *[a]

[a] *Department of Chemistry, Faculty of Science, National University of Singapore, Kent Ridge, 119260, Singapore. E-mail: chmandyh@nus.edu.sg*
[b] *Department of Chemistry, The Chinese University of Hong Kong, Shatin, N.T., Hong Kong*
[c] *Department of Chemistry, University of Waikato, Private Bag 3105, Hamilton, New Zealand*

Received 3rd August 1998, Accepted 16th November 1998

Three $\{Pd_3S_2\}$ aggregates, $[Pd_3Cl_2(\eta^2\text{-dppf})(\mu\text{-dppf})(\mu_3\text{-S})_2]$ and $[Pd_3Cl(\eta^2\text{-dppf})_2(PPh_3)(\mu_3\text{-S})_2]X$ [X = Cl or NO_3, dppf = 1,1′-bis(diphenylphosphino)ferrocene] have been synthesized from metal addition to a $\{Pd_2S_2\}$ molecular core in $[Pd_2(dppf)_2(\mu\text{-S})_2]$. X-Ray single-crystal crystallographic analysis revealed a common sulfide-bicapped triangle with insignificant Pd · · · Pd interactions. The former is neutral with a bridging and a chelating dppf ligand as well as two terminal chlorides. The dynamic behaviour has been studied by variable temperature ^{31}P and 2-D COSY NMR. A phosphine–chloride interchange and phosphine–phosphine exchanges enable the two dppf ligands to migrate around the Pd_3 plane. The solid-state structure corresponds to the static structure in solution at 198 K. The mixed phosphine complex **5a** (X = Cl) is ionic with two Pd–dppf chelating rings and a $\{Pd(PPh_3)Cl\}$ moiety. With a PPh_3 group taking up one site, it is stereochemically rigid. The other two complexes were studied by electrospray mass spectrometry (ESMS) in solution. The $\{Pd_3S_2\}$ core in the mixed phosphine (X = NO_3) is relatively stable to fragmentation under ESMS conditions.

Introduction

The use of ferrocenylphosphines as ligands in co-ordination chemistry is well known.[1] The ability of these ligands to convey the ferrocenyl qualities to the resultant complexes without disturbing the inherent characteristics of the latter has widened the scope of ferrocenyl complexes in the design of catalysts, drugs and materials. Although the metalloligand dppf [1,1′-bis(diphenylphosphino)ferrocene], which is probably the best developed ferrocenyl diphosphine, was first synthesized more than two decades ago, its chemical uniqueness and industrial importance were not fully appreciated until recently.[2] Some current initiatives are driven at the development of homoleptic complexes, *e.g.* $[M(dppf\text{-}P,P')_2]^+$ (M = Rh or Ir) and $[M_2(dppf\text{-}P,P')_2(\mu\text{-dppf})]^{2+}$ (M = Cu,[3,4] Ag[5] or Au[6]) and polymetallic aggregates[7] and clusters[8] comprising dppf. In this paper we shall focus on the co-ordination of dppf on a $\{Pd_3S_2\}$ core and study the structural and dynamic behaviour of the resultant complexes, namely $[Pd_3Cl_2(\eta^2\text{-dppf})(\mu\text{-dppf})(\mu_3\text{-S})_2]$ and $[Pd_3Cl(\eta^2\text{-dppf})_2(PPh_3)(\mu_3\text{-S})_2]X$ (X = Cl or NO_3). Our interest in the $\{Pd_2S_2\}$ and $\{Pd_3S_2\}$ cores dates back to our earlier work on the $\{Pt_2S_2\}$,[7] $\{Pt_2MS_2\}$[7] and $\{Pd_2S_2\}$[9] systems. The probability of two interconverting co-ordination modes of dppf on a metal core marks a scenario for positional isomerism. Similar behaviour has been elegantly described by Braunstein *et al.*[10] and other researchers[11] for PPh_3 and dppm complexes. This is the first report of the dynamic behaviour of dppf on a M_3 core.

Results and discussion

Synthesis and structures

Prior to our work, reports of the relevant palladium complexes are confined to the synthesis of $[Pd_2(PPh_3)_4(\mu\text{-S})_2]$[12] **1a**, $[Pd_3Cl_2(PPh_3)_4(\mu_3\text{-S})_2]$[13] **2** and $[Pd_3(PR_3)_6(\mu_3\text{-S})_2]^{2+}$ (PR_3 = PMe_3,[14] $PMePh_2$[14] or PEt_3[15]), **3**. Complex **1a** lacks spectroscopic and crystallographic support and its role as a precursor to the Pd_3 aggregates **2** and **3** has not been established. Recently $[Pd_2(dppe)_2(\mu\text{-S})_2]$ [dppe = 1,2-bis(diphenylphosphino)ethane] has been identified[16] and its metallation reactions reported.[17] The X-ray crystallographic analysis of **2** was carried out but no detailed data have been reported to date.[13] The addition reaction of $[Pd_2(dppf)_2(\mu\text{-S})_2]$ **1b** with $[PdCl_2(P\text{–}P)]$ (P–P = 2 × PPh_3 or diphosphines) does not result in the expected ionic complexes, $[Pd_3(dppf)_2(P\text{–}P)(\mu_3\text{-S})_2]Cl_2$, **6** or $[Pd_6(dppf)_4(\mu\text{-Cl})_2(\mu_3\text{-S})_4]Cl_2$, **7** but a trinuclear complex $[Pd_3Cl_2(\eta^2\text{-dppf})(\mu\text{-dppf})(\mu_3\text{-S})_2]$ **4**, losing all the P–P ligands. The PR_3 analogue of $[Pd_3(dppf)_2(P\text{–}P)(\mu\text{-S})_2]Cl_2$ is found in **3** whereas $[Pd_6(dppf)_4(\mu\text{-Cl})_2(\mu_3\text{-S})_4]Cl$, has an established platinum counterpart.[18] The molar ionic conductivity of **4** in MeOH is significantly lower than that expected for a 2:1 electrolyte. Although we can rule out an ionic model in the solid state (because of the shortage of ligands), there are several structural possibilities for **4** based on a neutral model. With two chloride and two dppf ligands distributed on a Pd_3 core, and the absence of any dangling phosphines (as verified by ^{31}P NMR), there are three obvious positional isomers (more if the *syn* and *anti* arrangements of the chlorides on neighbouring metals are included): (i) two terminal chlorides on a Pd atom and a chelating dppf on each of the remaining two (**I**); (ii) two terminal chlorides on two metal atoms bridged by a dppf ligand with the third metal bearing a dppf chelate (**II**); (iii) two terminal chlorides on two metals which are linked to the third metal through two dppf bridges (**III**). Isomers **I**, **II** and **III** thus have 0, 1 and 2 dppf bridges respectively. All three models can accommodate the 16-electron square-planar requirement for each palladium(II)

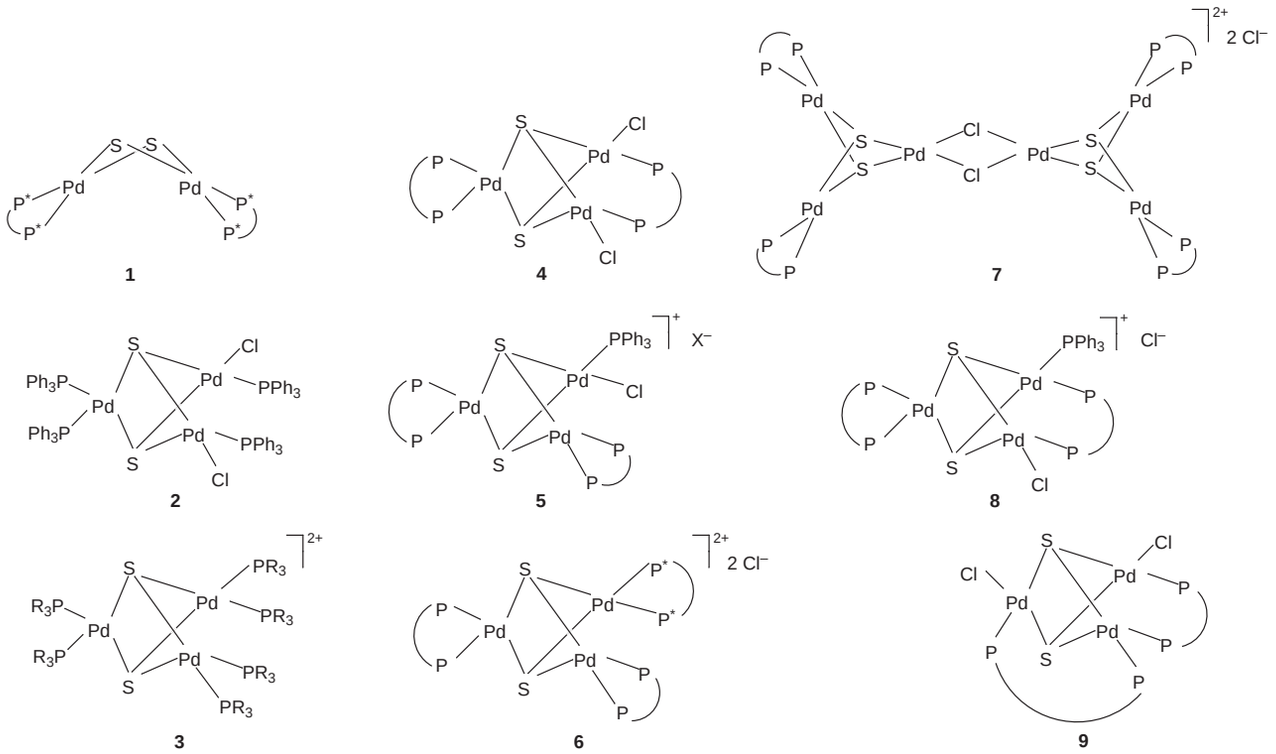

centre. An X-ray single-crystal crystallographic analysis of **4** (Fig. 1, Table 1) however revealed a structural model of **II** that can be considered as isostructural to **2**. It comprises a triangular plane of three d^8-Pd atoms capped above and below by two triply bridging sulfides in a $\{Pd_3S_2\}$ *TBPY* framework. Without significant Pd–Pd bonds [average 3.127(1) Å], the triangular core relies on the two capping sulfide ligands and a bridging dppf for support. All the Pd–S bonds [average 2.348(1) Å] *trans* to the Pd–P bonds are significantly lengthened by the higher *trans* influence of phosphine compared to those [average 2.277(2) Å] opposite the Pd–Cl bonds. The bridging Pd–P bonds [2.290(2) Å] are significantly shorter, and presumably stronger than the chelating Pd–P bonds [2.320(1) Å]. This imbalance is not surprising in view of the large bite size of dppf, especially on a square-planar metal [P(1)–Pd(1)–P(2) 100.8(1)° is hence significantly greater than the ideal 90°], and could provide an additional driving force for the fluxionality described later.

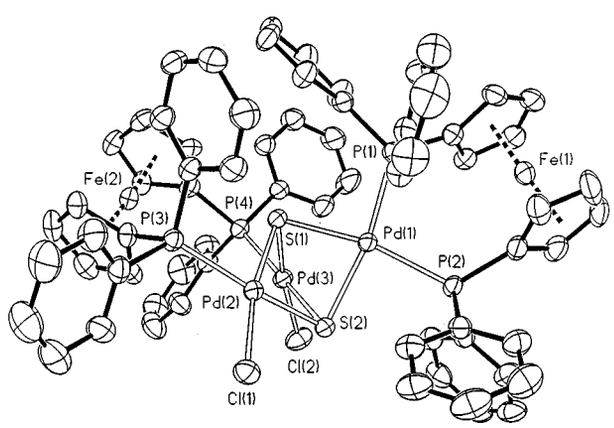

Fig. 1 An ORTEP[19] plot (30% thermal ellipsoids) of the molecular structure of $[Pd_3Cl_2(\eta^2\text{-dppf})(\mu\text{-dppf})(\mu_3\text{-S})_2]$ **4** with solvate removed for clarity.

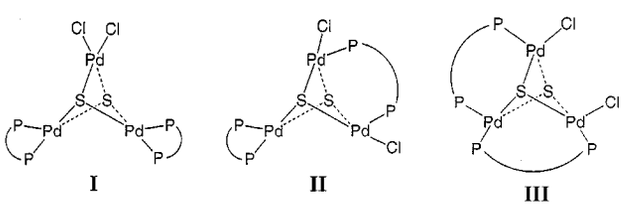

Attempts to explore the heterometallic chemistry of complex **1b** with $[HgCl_2(PPh_3)_2]$ and $[Cu(NO_3)(PPh_3)]$ surprisingly led to the isolation of two homometallic products, $[Pd_3Cl(\eta^2\text{-dppf})_2(PPh_3)(\mu_3\text{-S})_2]X$ (X = Cl **5a** or NO_3 **5b**), which share the same cation and are isostructural. Complex **5a** is best synthesized from **1b** and $[PdCl_2(PPh_3)_2]$ or $[Pd_2Cl_2(PPh_3)_2(\mu\text{-Cl})_2]$ although **4** is an inevitable by-product. The ^{31}P NMR analysis confirmed that **4** in the presence of free PPh_3 gives rise to **5a** (and other presently unidentified products). Conductivity measurements suggest both **5a** and **5b** are 1 : 1 electrolytes in solution. X-Ray single-crystal crystallographic analyses of **5a** and **5b** [Fig. 2(a) and 2(b)] reveal two similar *TBPY* frameworks each of which is made up of two {Pd(dppf)} and one {PdCl(PPh_3)} moieties linked solely by the sulfide ligands. This structure is related to the $\{PdPt_2\}$ complex isolated by Mingos and co-workers.[18] The isosceles metal triangle has a Pd···Pd edge [3.2032(7) and 3.2383(8) Å in **5a** and **5b** respectively] which is significantly longer than the remaining two [average 3.0751(7) and 3.0895(8) Å in **5a** and **5b**]. This is indicative of the steric repulsion between the two dppf-bearing palladium moieties. Among the six Pd–S bonds, one [Pd(3)–S(2)] is uniquely short and presumably strong [2.297(2) and 2.287(2) Å compared to the rest, *viz.* average 2.344(2) and 2.348(2) Å in **5a** and **5b**] because it avoids a *trans*-directing phosphine. The Pd–P (PPh_3) bond [2.295(2) and

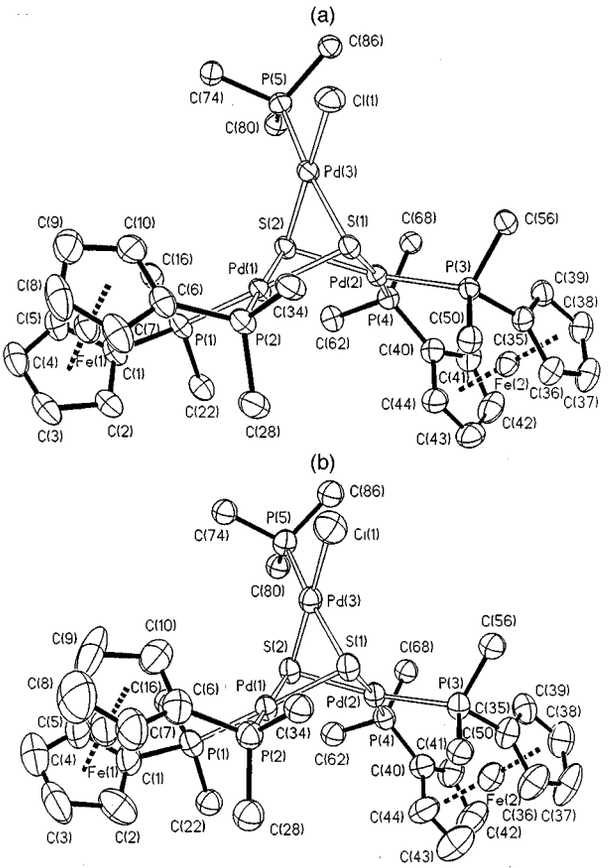

Fig. 2 The ORTEP plots (35% thermal ellipsoids) of the molecular structures of $[Pd_3Cl(\eta^2\text{-dppf})_2(PPh_3)(\mu_3\text{-}S)_2]X$ [X = Cl **5a** (a) or NO_3 **5b** (b)].

2.299(2) Å] is significantly shorter than the Pd–P (dppf) bonds [average 2.320(2) and 2.328(2) Å in **5a** and **5b** respectively]. This is reminiscent of the slight strain experienced by a dppf chelate.

Electrospray mass spectrometry

The ESMS spectra of complex **4** were recorded in MeCN and MeOH solutions. Since **4** is electrically neutral, the expected ionisation pathways would reasonably be expected to be loss of a chloride ligand[20] and/or oxidation of one of the ferrocene groups.[21] The ion $[\mathbf{4} - Cl]^+$ (*m/z* 1527) was not observed, however the ion $[\mathbf{4} - Cl + MeCN]^+$, *i.e.* $[Pd_3Cl(dppf)_2(MeCN)(\mu\text{-}S)_2]^+$, was observed at *m/z* 1568 as a low intensity ion in MeCN solvent at a cone voltage of 20 V. However, for **4** the fragment ions $[PdCl(dppf)]^+$ (*m/z* 695) and $[Pd_2Cl_3(dppf)_2]^+$ (*m/z* 1428) were the two most intense ions observed in MeOH at a cone voltage of 40 V. Addition of pyridine to the ESMS solution gave the species $[PdCl(dppf)(py)]^+$ at *m/z* 774 and at a cone voltage of 20 V, while at a higher cone voltage (50 V) the pyridine was lost, as expected, giving $[PdCl(dppf)]^+$.

The ESMS spectra of cationic complex **5b** recorded in MeCN and MeOH solutions were more informative, as expected for a pre-existing cationic species. The parent cation of **5b**, $[M]^+$, is observed at *m/z* 1789 at a range of cone voltages, from 5 to 60 V; the assignment was confirmed by agreement between the observed and calculated isotope patterns, and the *m/z* 1 separation between adjacent peaks indicating a singly charged cation. At 60 V, $[M]^+$ was the dominant species observed. At lower cone voltages, dicationic species were also major ions, *e.g.* the base peak was $[M - Cl]^{2+}$ at 20 V with the *m/z* 0.5 separation of peaks in the isotope pattern confirming the 2+ charge (Fig. 3). At a cone voltage of 5 V the solvated species $[M - Cl + MeCN]^{2+}$ (*m/z* 898) was the base peak, formed from adventitious MeCN in the spectrometer and ancillary solvent delivery system. Other ions $[M - Cl]^{2+}$, $[M - Cl + H_2O]^{2+}$ and $[M - Cl + MeOH]^{2+}$ were also observed as weak peaks. The $[M - Cl + MeCN]^{2+}$ ion presumably forms since the $[M - Cl]^{2+}$ cation has a vacant co-ordination site available upon loss of chloride from $[M]^+$. The ion $[M - Cl + MeCN]^{2+}$ was only very minor at 20 V indicating that the MeCN ligand is easily lost. The assignment was confirmed when comparison was made with the ESMS spectrum of the complex in MeCN solvent at a cone voltage of 20 V, whereupon the $[M - Cl + MeCN]^{2+}$ ion was the major dicationic species observed. Additionally, it is noted that the $[M]^+$ cation has all palladium atoms four-co-ordinate, and so will have little tendency to co-ordinate a MeCN ligand, and thus no significant $[M + MeCN]^+$ ion was observed, even under optimum conditions (MeCN solvent, and low cone voltage of 5 V).

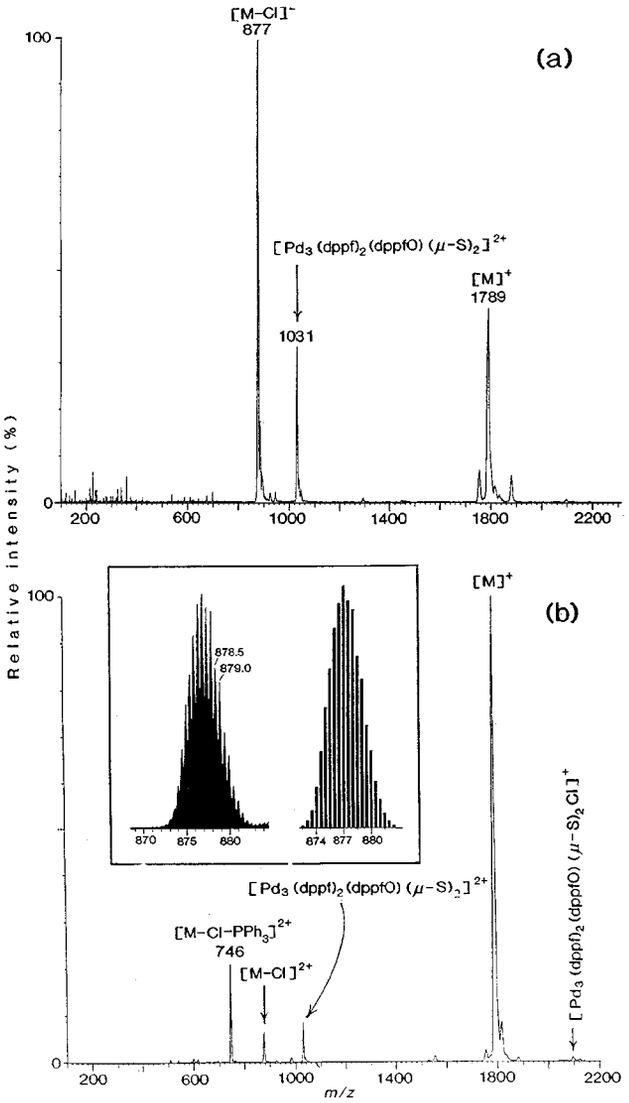

Fig. 3 Positive-ion electrospray mass spectra of the complex $[Pd_3Cl(\eta^2\text{-dppf})_2(PPh_3)(\mu_3\text{-}S)_2]NO_3$ **5b** $(= M^+NO_3^-)$ recorded in MeOH solution: (a) at a cone voltage of 20 V, showing the ion $[M - Cl]^{2+}$ as the base peak; (b) at a cone voltage of 60 V, showing $[M]^+$ as the base peak and some loss of the PPh_3 ligand giving the ion $[M - Cl - PPh_3]^{2+}$. The insert to (b) shows a comparison of the experimental isotope pattern (left) of the $[M - Cl]^{2+}$ ion (recorded at 40 V) and the calculated pattern (right) for this ion; the *m/z* 0.5 separation of adjacent peaks is the signature of a dication.

An additional relatively weak ion at *m/z* 1031 was shown to be a dication from its isotope distribution pattern. A possible assignment for this species is $[Pd_3(dppf)_2(dppfO)(\mu\text{-}S)_2]^{2+}$. This species can be formed from **5b** by displacement of the co-ordinated PPh_3 ligand by the monooxide of dppf (dppfO), and loss of the chloride ligand (as observed for **5b** itself). Support for this assignment comes from the observation of a low inten-

Table 1 Selected bond distances (Å) and angles (°)

(a) $[Pd_3Cl_2(\eta^2\text{-dppf})(\mu\text{-dppf})(\mu_3\text{-S})_2]$ **4**

Pd(1)–S(1)	2.329(1)	Pd(1)–S(2)	2.346(1)	Pd(2)–P(3)	2.294(2)	Pd(2)–Cl(1)	2.353(2)
Pd(2)–S(1)	2.274(1)	Pd(2)–S(2)	2.349(2)	Pd(3)–P(4)	2.285(1)	Pd(3)–Cl(2)	2.352(2)
Pd(3)–S(1)	2.280(2)	Pd(3)–S(2)	2.369(1)	Pd(1) · · · Pd(2)	3.132(1)	Pd(1) · · · Pd(3)	3.117(1)
Pd(1)–P(1)	2.316(1)	Pd(1)–P(2)	2.323(1)	Pd(2) · · · Pd(3)	3.132(1)		
S(1)–Pd(1)–S(2)	77.5(1)	S(1)–Pd(2)–S(2)	78.6(1)	Cl(1)–Pd(2)–S(1)	168.1(1)	Cl(1)–Pd(2)–S(2)	95.2(1)
S(1)–Pd(3)–S(2)	78.0(1)	P(1)–Pd(1)–P(2)	100.8(1)	Cl(2)–Pd(3)–S(1)	171.7(1)	Cl(2)–Pd(3)–S(2)	95.2(1)
P(1)–Pd(1)–S(1)	91.3(1)	P(1)–Pd(1)–S(2)	168.6(1)	Cl(1)–Pd(2)–P(3)	98.8(1)	Cl(2)–Pd(3)–P(4)	93.6(1)
P(2)–Pd(1)–S(1)	167.7(1)	P(2)–Pd(1)–S(2)	90.3(1)	Pd(1)–S(1)–Pd(2)	85.8(1)	Pd(1)–S(1)–Pd(3)	85.1(1)
P(3)–Pd(2)–S(1)	88.8(1)	P(3)–Pd(2)–S(2)	164.4(1)	Pd(2)–S(1)–Pd(3)	86.9(1)	Pd(1)–S(2)–Pd(2)	83.7(1)
P(4)–Pd(3)–S(1)	93.4(1)	P(4)–Pd(3)–S(2)	170.9(1)	Pd(1)–S(2)–Pd(3)	82.7(1)	Pd(2)–S(2)–Pd(3)	83.2(1)

(b) $[Pd_3Cl(\eta^2\text{-dppf})_2(PPh_3)(\mu_3\text{-S})_2]Cl$ **5a**

Pd(1)–S(1)	2.3167(14)	Pd(1)–S(2)	2.362(2)	Pd(2)–P(3)	2.321(2)	Pd(2)–P(4)	2.324(2)
Pd(2)–S(1)	2.351(2)	Pd(2)–S(2)	2.340(2)	Pd(3)–P(5)	2.295(2)	Pd(3)–Cl(1)	2.340(2)
Pd(3)–S(1)	2.350(2)	Pd(3)–S(2)	2.297(2)	Pd(1) · · · Pd(2)	3.2032(7)	Pd(1) · · · Pd(3)	3.0572(6)
Pd(1)–P(1)	2.310(2)	Pd(1)–P(2)	2.323(2)	Pd(2) · · · Pd(3)	3.0929(7)		
S(1)–Pd(1)–S(2)	79.03(5)	S(1)–Pd(2)–S(2)	78.78(5)	P(4)–Pd(2)–S(2)	92.62(6)	P(5)–Pd(3)–S(1)	172.23(6)
S(1)–Pd(3)–S(2)	79.67(5)	P(1)–Pd(1)–P(2)	100.99(6)	P(5)–Pd(3)–S(2)	98.71(6)	Cl(1)–Pd(3)–S(1)	90.81(6)
P(3)–Pd(2)–P(4)	101.61(6)	P(1)–Pd(1)–S(1)	167.58(6)	Cl(1)–Pd(3)–S(2)	168.52(7)	Cl(1)–Pd(3)–P(5)	91.57(7)
P(1)–Pd(1)–S(2)	88.82(5)	P(2)–Pd(1)–S(1)	91.34(5)	Pd(1)–S(1)–Pd(2)	86.66(5)	Pd(1)–S(1)–Pd(3)	81.85(5)
P(2)–Pd(1)–S(2)	169.10(6)	P(3)–Pd(2)–S(1)	87.02(5)	Pd(2)–S(1)–Pd(3)	82.27(5)	Pd(1)–S(2)–Pd(2)	85.87(5)
P(3)–Pd(2)–S(2)	164.80(6)	P(4)–Pd(2)–S(1)	171.37(6)	Pd(1)–S(2)–Pd(3)	82.01(5)	Pd(2)–S(2)–Pd(3)	83.67(5)

(c) $[Pd_3Cl(\eta^2\text{-dppf})_2(PPh_3)(\mu_3\text{-S})_2]NO_3\cdot CH_2Cl_2$ **5b**

Pd(1)–S(1)	2.326(2)	Pd(1)–S(2)	2.360(2)	Pd(2)–P(3)	2.333(2)	Pd(2)–P(4)	2.326(2)
Pd(2)–S(1)	2.357(2)	Pd(2)–S(2)	2.343(2)	Pd(3)–P(5)	2.299(2)	Pd(3)–Cl(1)	2.354(2)
Pd(3)–S(1)	2.354(2)	Pd(3)–S(2)	2.287(2)	Pd(1) · · · Pd(2)	3.2383(8)	Pd(1) · · · Pd(3)	3.0923(8)
Pd(1)–P(1)	2.333(2)	Pd(1)–P(2)	2.318(2)	Pd(2) · · · Pd(3)	3.0867(8)		
S(1)–Pd(1)–S(2)	78.08(6)	S(1)–Pd(2)–S(2)	77.81(6)	P(4)–Pd(2)–S(2)	93.66(7)	P(5)–Pd(3)–S(1)	172.16(7)
S(1)–Pd(3)–S(2)	78.96(6)	P(1)–Pd(1)–P(2)	98.34(7)	P(5)–Pd(3)–S(2)	97.59(7)	Cl(1)–Pd(3)–S(1)	93.54(8)
P(3)–Pd(2)–P(4)	100.42(7)	P(1)–Pd(1)–S(1)	169.80(7)	Cl(1)–Pd(3)–S(2)	170.60(8)	Cl(1)–Pd(3)–P(5)	90.53(8)
P(1)–Pd(1)–S(2)	91.94(7)	P(2)–Pd(1)–S(1)	91.79(6)	Pd(1)–S(1)–Pd(2)	87.51(6)	Pd(2)–S(1)–Pd(3)	81.88(5)
P(2)–Pd(1)–S(2)	168.53(7)	P(3)–Pd(2)–S(1)	88.22(6)	Pd(1)–S(2)–Pd(2)	87.04(6)	Pd(1)–S(2)–Pd(3)	83.41(6)
P(3)–Pd(2)–S(2)	165.05(7)	P(4)–Pd(2)–S(1)	171.32(6)	Pd(2)–S(2)–Pd(3)	83.61(6)		

sity ion at *ca. m*/*z* 2097, consistent with $[Pd_3Cl(dppf)_2(dppfO)(\mu\text{-S})_2]^+$, which is a direct analogue of **5b**, with the PPh_3 ligand replaced by monodentate dppfO. The formation of phosphine oxide species by oxidation in ESMS has been observed previously,[22] and could account for the formation of a small amount of dppfO (subsequently co-ordinated to palladium) in the present case. Dissociation of one of the PPh_2 from a η^2-dppf ligand, followed by oxidation of this group, could provide a possible mechanism for its formation.

When the spectrum of complex **5b** is recorded at the relatively high cone voltage of 60 V an ion at *m*/*z* 746 is observed, which is also a dication from the isotope pattern. This species is readily identified as the ion formed by loss of the monodentate PPh_3 ligand, *i.e.* $[M - Cl - PPh_3]^{2+}$. The loss of neutral monodentate ligands is a common feature of fragmentation pathways of co-ordination complexes in ESMS under higher cone voltages.

The results obtained for complex **5b** above suggest that the Pd_3S_2 core is relatively stable to fragmentation under ESMS conditions. The ESMS data should be considered in conjunction with those from other techniques such as NMR spectroscopy.

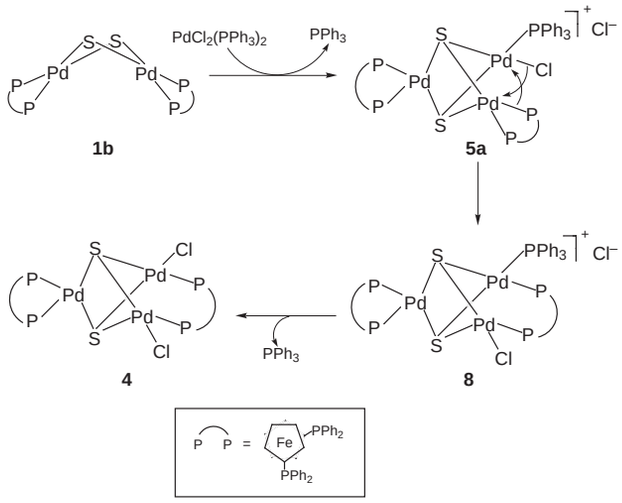

Scheme 1 A possible formation pathway for $[Pd_3Cl_2(\eta^2\text{-dppf})(\mu\text{-dppf})(\mu_3\text{-S})_2]$ **4**.

NMR and fluxionality

Formation of complex **4** is likely to follow a general pathway similar to those of the platinum analogues,[7] *viz*. addition of an acidic {PdCl(PPh_3)} moiety to the basic metalloligand **1b** giving **5a** which undergoes a chloride–phosphine interchange in a positional isomerization process to give $[Pd_3Cl(\eta^2\text{-dppf})(\mu\text{-dppf})(PPh_3)(\mu_3\text{-S})_2]Cl$ **8**. Chloride displacement of phosphine would give the final product **4** (Scheme 1). The presence of **5a** (see later) in the reaction mixture is verified by ^{31}P NMR analysis. Complex **5a** decomposes slowly to give **4** in a donor solvent like thf. The formation of **4** from **5a** is reversible upon addition of an excess of PPh_3. The {$PdPt_2$} equivalent of **8**, *viz*. $[PdPt_2Cl(PPh_3)_5(\mu_3\text{-S})_2]Cl$,[18] has been reported. Such ease of conversion for dppf from chelating to bridging mode and chloride migration on the Pd_3 core prompted us to look for the positional isomers at different temperatures.

At 300 K the ^{31}P NMR spectrum of complex **4** comprises a quartet at δ 23.01 and a doublet at δ 26.04 (Fig. 4). A very broad signal at high field ($\approx \delta$ 17) is barely discernible. Although these three signals (if the latter signal is included) can be anticipated from the solid-state structure described earlier, the

coupling pattern is inconsistent with the static form of such a structure. At 273 K the high-field peak emerges as two discrete peaks at δ 18.19 and 15.51 which readily sharpen as two doublets at 243 K. Fine splitting of the resonance at δ 15.51 into doublets of a doublet is also apparent. The low-field peaks (δ 23.01 and 26.04) broaden as the temperature is lowered but eventually re-emerge as a multiplet at δ 21.89 and a doublet at δ 26.46.

Two possible fluxional mechanisms are depicted in Scheme 2 (Path a and b). Path a involves a "slug-style" motion in which two dppf ligands travel around the ring in a synchronized manner whereby they interchange between two co-ordination modes, chelating and bridging. It is well established that dppf commonly takes up such modes.[2] However, this movement would effectively equilibrate all the phosphines and is hence inconsistent with the room temperature (r.t.) spectrum observed. An alternative motion (Path b) relies on the intercalation of the chloride–phosphine and phosphine–phosphine exchanges. This effectively generates a unique phosphine (P_A) above the plane, and three equivalent phosphines ($P_{B\text{-}D}$) below the plane, which is consistent with the r.t. spectrum. In this pathway (Path b) a series of positional isomers (*e.g.* **9**) are generated whereby both dppf ligands are in a bridging mode. These isomers can go through other forms of fluxionalities, for example by chelate–bridge exchange or "screen wiper"-type movement of a dppf bridge whizzing around the three palladium corners. However, the possibility of two isomers coexisting is dismissed by a ^{31}P COSY NMR analysis. A spectrum measured at 205 K (Fig. 5) clearly suggests that the quartet-like resonance at δ 21.83 is strongly coupled to all (three) other resonances. This also explains the doublet features of the other peaks that are

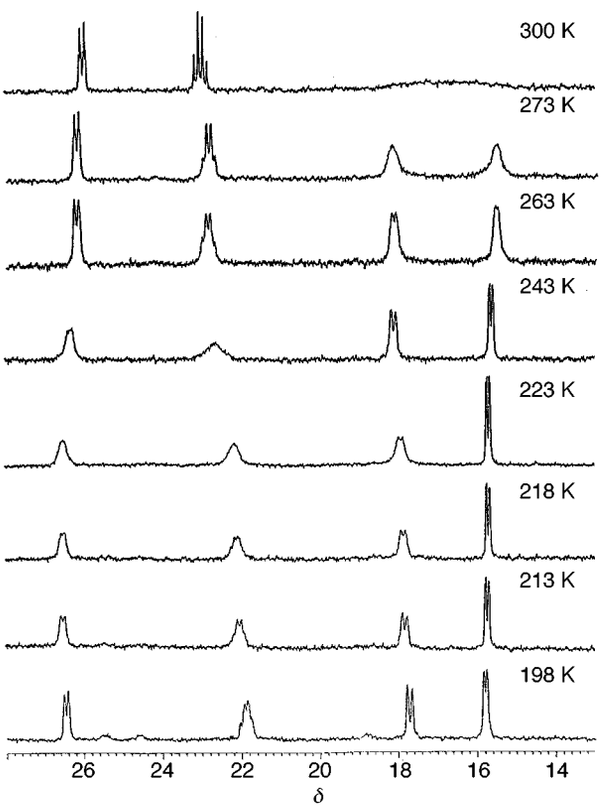

Fig. 4 ^{31}P-{H} Variable temperature (198–300 K) NMR spectra (202.46 MHz) of $[Pd_3Cl_2(\eta^2\text{-dppf})(\mu\text{-dppf})(\mu_3\text{-S})_2]$ **4** in CD_2Cl_2.

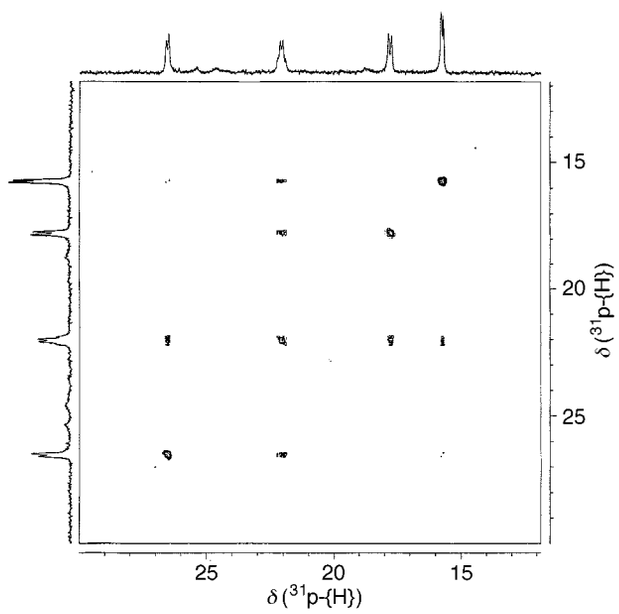

Fig. 5 ^{31}P-{H} 2-D COSY NMR Spectrum (202.46 MHz) of $[Pd_3Cl_2(\eta^2\text{-dppf})(\mu\text{-dppf})(\mu_3\text{-S})_2]$ **4** in CD_2Cl_2 at 205 K.

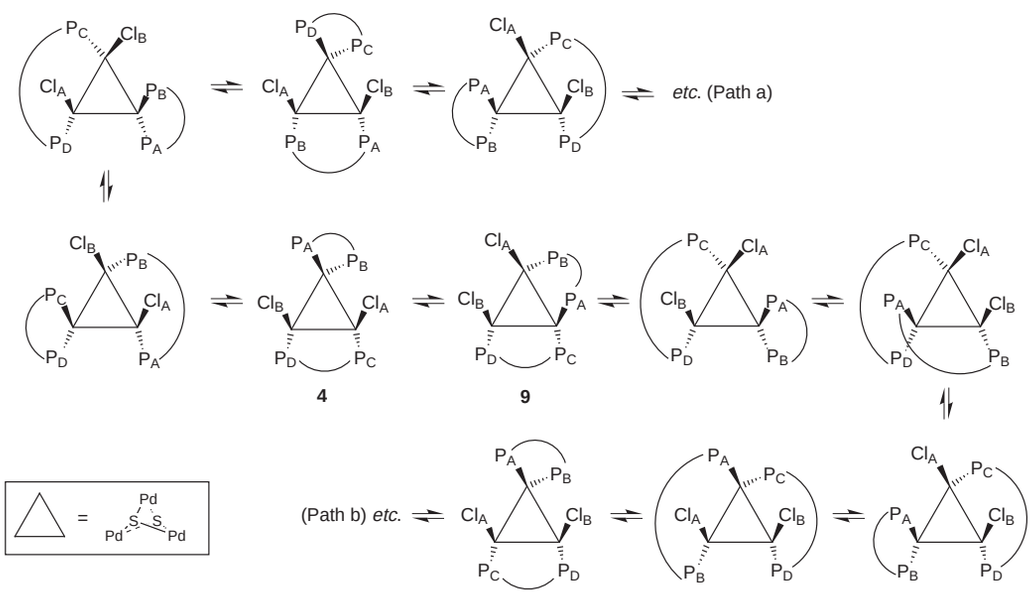

Scheme 2 Two possible fluxional mechanisms for $[Pd_3Cl_2(\eta^2\text{-dppf})(\mu\text{-dppf})(\mu_3\text{-S})_2]$ **4** whereby a series of positional isomers are formed from a rapid interchange of bridging and chelating diphosphines (Path a) and interchange of chloride–phosphine and phosphine–phosphine exchanges (Path b). Variable temperature and COSY ^{31}P NMR results are consistent with Path b.

not related to each other. These support **4** as the sole species in solution and its fluxional mechanism is depicted in Path b of Scheme 2. The solid-state structure of **4** is captured as the static structure in solution at 198 K. Steric crowding due largely to the phenyl rings restricts the Pd–P bond rotation and distinguishes P_C and P_D, which correspond to the two high-field peaks (referring to structure **4** in Scheme 2). Their lack of mutual coupling is understood based on the lack of direct Pd–Pd interactions as they are four bonds apart. Coupling between P_A and P_B is expected since they are related by chelation. Long-range coupling of P_B with P_C and P_D is facilitated by their sharing of the same *trans* ligand, which is the sulfide atom above the Pd_3 ring. The strong coupling of ligands *trans* to each other and the effective spin transfer *via* sulfide is a common feature in these square-planar d^8 sulfide complexes.[18,23] It is evident that such $^4J(P_BP_{C/D})$ coupling is of similar magnitude to $^2J(P_AP_B)$ coupling. This also explains the quartet-like appearance of P_B which strictly should be seen as doublets of doublets of a doublet.

With a stable PPh_3 occupying one site of the palladium triangle in complex **5**, the phosphine mobility seen in **4** is therefore destroyed. The observed first-order A_2B_2X spectra containing three discrete resonances are consistent with the solid-state structures (the phosphines above and below the metal plane are inequivalent because of asymmetry on the palladium site that carries the PPh_3 ligand). Spin–spin coupling is observed between the phosphine sites on a chelate [^2J(P–P) 22 Hz], and between the dppf and PPh_3 phosphines [^4J(P–P) 17 Hz], at a *syn* orientation. With a terminal PPh_3 occupying one site and the lack of entropic drive for PPh_3 to migrate among the palladium atoms, the impetus for fluxionality observed in **4** and **9** is lost and the complex, not surprisingly, is stereochemically rigid. While the key features of the NMR spectra of **5a** and **5b** are essentially maintained, the PPh_3 resonance of **5b** is slightly deshielded (by ≈0.4 ppm) compared to that of **5a**. We attribute this to a rapid exchange of chloride and nitrate in solution that affects the PPh_3 shift most as it occurs on the PPh_3-bearing palladium centre.

Conclusion

Results in this work suggested that there are as many distinctive structures between the palladium and platinum analogues as there are common ones. The molecular fluxionality arising from the introduction of a diphosphine such as dppf to the Pd_3 core is reminiscent of a combination of factors, namely (i) the kinetic lability of phosphine on Pd^{II}, (ii) the ability of sulfide to keep the Pd_3 triangle intact while other ligands dissociate and migrate, (iii) migration of a diphosphine through an interchange of chelating and bridging modes and (iv) facility of phosphine–chloride and phosphine–phosphine exchanges on the metal plane. It is especially surprising that such a bulky diphosphine appears to exhibit little resistance in whizzing around the Pd_3 triangle.

Experimental

General

All reactions were routinely performed under a pure argon atmosphere unless otherwise stated. All solvents were distilled and degassed before use. Elemental analyses were performed by the microanalytical laboratory of the Department of Chemistry at the National University of Singapore. All NMR spectra were recorded on a Bruker ACF 300 spectrometer with the exception of variable temperature and 2-D COSY NMR analyses which were carried out on a Bruker AMX 500 spectrometer. The ^{31}P NMR chemical shifts are externally referenced to 85% H_3PO_4. Infrared spectra were recorded on a Perkin-Elmer 1600 FT-IR spectrophotometer. Conductivity was determined by using a STEM Conductivity 1000 meter.

Syntheses

$[Pd_3Cl_2(\eta^2\text{-dppf})(\mu\text{-dppf})(\mu_3\text{-S})_2]\cdot 2CH_2Cl_2$ 4. A mixture of $[Pd_2(dppf)_2(\mu\text{-S})_2]$ **1b** (0.10 g, 0.072 mmol) and $[PdCl_2(PPh_3)_2]$ (0.051 g, 0.072 mmol) was suspended in THF (20 ml) and stirred for a day at r.t. The resultant red suspension was filtered and the residue extracted by CH_2Cl_2 (20 ml). Slow crystallization upon addition of hexane and subsequent recrystallization from CH_2Cl_2–hexane gave orange-red crystals of $[Pd_3Cl_2(\eta^2\text{-dppf})(\mu\text{-dppf})(\mu_3\text{-S})_2]\cdot 2CH_2Cl_2$. Yield: 0.065 g (52%) (Found: C, 48.14; H, 3.39; Fe, 5.76; P, 6.79; Pd, 16.73; S, 3.81. Calc.: C, 48.49; H, 3.46; Fe, 6.47; P, 7.16; Pd, 18.43; S, 3.69%). ^1H NMR ($CDCl_3$): δ 8.20–7.11 (m, 40 H, C_6H_5), 4.52 (s, 4 H, C_5H_4), 4.21 (s, 4 H, C_5H_4) and 4.14 (s, 4 H, C_5H_4). ^{31}P NMR ($CDCl_3$) (298 K): δ 25.1 [dd, J(P–P) 22.5 and 6.5], 22.2 [q, J(P–P) 21.6 Hz] and 16.3 (br). Λ_m (10^{-3} M) 19.6 Ω^{-1} cm^2 mol^{-1} (CH_3OH).

$[Pd_3Cl(\eta^2\text{-dppf})_2(PPh_3)(\mu_3\text{-S})_2]Cl$ 5a. A mixture of complexes **1b** (0.031 g, 0.0224 mmol) and $[PdCl_2(PPh_3)_2]$ (0.016 g, 0.0224 mmol) {$[Pd_2Cl_2(PPh_3)_2(\mu\text{-Cl})_2]$ can also be used} was suspended in MeOH (20 ml) and stirred for a day at r.t. to give a reddish brown suspension. The resultant mixture was filtered and the filtrate precipitated with diethyl ether to give a crude sample of **5a** with **4** as a possible by-product. Recrystallization of the product from a mixture of MeOH–diethyl ether gave red crystals of $[Pd_3Cl(\eta^2\text{-dppf})_2(PPh_3)(\mu_3\text{-S})_2]Cl$. Yield: 0.014 g (34%). The same complex was originally prepared from **1b** and $[HgCl_2(PPh_3)_2]$ in THF at r.t. (Found: C, 56.25; H, 4.32; Cl, 3.44; Pd, 14.23; S, 3.65. Calc.: C, 56.58; H, 3.89; Cl, 3.89; Pd, 17.50; S, 4.21%). ^1H NMR ($CDCl_3$): δ 7.59–6.79 (m, 40 H, C_6H_5), 4.41, 4.21 and 4.04. ^{31}P NMR ($CDCl_3$): δ 25.5 (m), 23.2 [t, ^2J(P–P) 22.3] and 22.1 [t, ^4J(P–P) 17.0 Hz]. Λ_m (10^{-3} M) 85.2 Ω^{-1} cm^2 mol^{-1} (CH_3OH).

$[Pd_3Cl(\eta^2\text{-dppf})_2(PPh_3)(\mu_3\text{-S})_2]NO_3\cdot CH_2Cl_2$ 5b. A mixture of complexes **1b** (0.14 g, 0.1 mmol) and $[Cu(NO_3)(PPh_3)_2]$ (0.065 g, 0.1 mmol) was suspended in THF (20 ml) and stirred for one day at r.t. The resultant red suspension was filtered and the residue extracted using CH_2Cl_2 (20 ml). Evaporation to a crude residue followed by recrystallization from a mixture of CH_2Cl_2–hexane gave red crystals of $[Pd_3Cl(\eta^2\text{-dppf})_2(PPh_3)(\mu_3\text{-S})_2]NO_3\cdot CH_2Cl_2$. Yield: 0.043 g (33%) (Found: C, 53.52; H, 3.92; Fe, 5.37; N, 0.82; P, 9.71; Pd, 13.10; S, 3.35. Calc.: C, 53.95; H, 3.77; Fe, 5.79; N, 0.72; P, 8.01; Pd, 16.49; S, 3.31%). ^1H NMR (CD_2Cl_2): δ 7.47–7.13 (m, 40 H, C_6H_5), 4.47 (s, 4 H, C_5H_4), 4.40 (s, 8 H, C_5H_4), 4.34 (s, 4 H, C_5H_4) and 4.02 (s, 8 H, C_5H_4). ^{31}P NMR ($CDCl_3$): δ 24.9 (m), 23.4 [t, ^4J(P–P) 17.2] and 22.5 [t, ^2J(P–P) 21.8 Hz]. Λ_m (10^{-3} M) 78.8 Ω^{-1} cm^2 mol^{-1} (CH_3OH). IR (KBr): 1384.1 cm^{-1} (unco-ordinated NO_3^-). Similar to **5a**, Cu may be eliminated as sulfide-containing materials.

Crystal structure determination and refinement

Suitable crystals of $[Pd_3Cl_2(dppf)_2(\mu_3\text{-S})_2]$ **4** and $[Pd_3Cl(\eta^2\text{-dppf})_2(PPh_3)(\mu_3\text{-S})_2]X$ (X = Cl **5a** or NO_3 **5b**) for structure determination were obtained by layering a CH_2Cl_2 solution of each compound with hexane under an argon atmosphere. The crystals used for analysis were of dimensions 0.2 × 0.2 × 0.5, 0.2 × 0.2 × 0.3 and 0.1 × 0.3 × 0.4 mm, respectively.

Intensity data were collected at 294 K on a MSC/Rigaku RAXIS IIC imaging-plate diffractometer[24] using graphite-monochromatized Mo-Kα radiation (λ = 0.7103 Å) from a rotating-anode generator operating at 50 kV and 90 mA. A self-consistent semiempirical absorption correction based on Fourier coefficient fitting of symmetry-equivalent reflections was applied using the ABSCOR program.[25] The crystal structures were determined by the direct method. The discrete chloride ion in complex **5a** is badly disordered over multiple sites, and its scattering is accounted for by atoms Cl(2) to Cl(8) with assigned fractional site occupancy factors. The nitrate ion in **5b** is likewise disordered and modeled by oxygen atoms O(1) to

O(11) with partial site occupancies. All other non-hydrogen atoms were refined using anisotropic thermal parameters. Hydrogen atoms were all generated geometrically (C–H bond lengths fixed at 0.96 Å), assigned appropriate isotropic thermal parameters and allowed to ride on their parent carbon atoms. All the H atoms were held stationary and included in the structure factor calculation in the final stage of full-matrix least-squares refinement. Computation was performed on an IBM compatible 486 PC with the Siemens SHELXTL PC version 5.03 program package[26] for compound **4** and the SHELXL 93 least-squares program[27] for **5a** and **5b**. Refinement of $wR2$ was based on F^2 for all reflections except for n with very negative F^2 or flagged for potential systematic errors. A conventional $R1$ based on observed F greater than $4\sigma(F_o)$ was also calculated for comparison.

Crystal data. $C_{68}H_{56}Cl_2Fe_2P_4Pd_3S_2$ **4**, $M = 1562.90$, monoclinic, space group Cc (no. 9), $a = 21.084(1)$, $b = 20.223(1)$, $c = 19.088(1)$ Å, $\beta = 122.32(1)°$, $U = 6878(3)$ Å^3, $T = 294$ K, $Z = 4$, μ(Mo-Kα) = 1.450 mm^{-1}, 13194 reflections measured, 9925 unique ($R_{int} = 0.0177$) which were used in calculations. The final $wR(F^2)$ was 0.0382, $R1 = 0.0337$.

$C_{86}H_{71}Cl_2Fe_2P_5Pd_3S_2$ **5a**, $M = 1825.20$, monoclinic, space group $P2_1/c$ (no. 14), $a = 13.323(1)$, $b = 25.599(1)$, $c = 26.106(1)$ Å, $\beta = 103.63(1)°$, $U = 8652.8(8)$ Å^3, $T = 293(2)$ K, $Z = 4$, μ(Mo-Kα) = 1.182 mm^{-1}, 29102 reflections measured, 16143 unique ($R_{int} = 0.0433$) which were used in calculations. The final $wR(F^2)$ was 0.2099, $R1 = 0.0663$.

$C_{86}H_{71}ClFe_2NO_3P_5Pd_3S_2$ **5b**, $M = 1851.76$, triclinic, space group $P\bar{1}$ (no. 2), $a = 14.842(1)$, $b = 17.231(1)$, $c = 17.478(1)$ Å, $a = 76.46(1)$, $\beta = 88.78(1)$, $\gamma = 87.65(1)°$, $U = 4341.7(5)$ Å^3, $T = 293(2)$ K, $Z = 2$, μ(Mo-Kα) = 1.152 mm^{-1}, 14846 reflections measured, 14846 unique ($R_{int} = 0.0000$) which were used in calculations. The final $wR(F^2)$ was 0.2137, $R1 = 0.0703$.

CCDC reference number 186/1255.

Electrospray mass spectroscopy

Electrospray mass spectra were recorded in positive-ion mode using a VG Platform II instrument, in either methanol or acetonitrile as the mobile phase. Further experimental details are given elsewhere.[21a] Theoretical isotope patterns were obtained using the ISOTOPE program.[28]

Acknowledgements

The authors acknowledge the National University of Singapore (NUS) (Grant RP950695) for financial support, Y. P. Leong for assistance in the preparation of this manuscript and S. Y. Wong for technical assistance. J. S. L. Y. and G. L. thank NUS for a research scholarship. W. H. thanks the University of Waikato and the New Zealand Lottery Grants Board for financial assistance, and W. Jackson for technical support.

References

1 W. R. Cullen and J. D. Woollins, *Coord. Chem. Rev.*, 1981, **39**, 1; T. Hayashi and M. Kumada, *Acc. Chem. Res.*, 1982, **15**, 395; W. R. Cullen, S. J. Rettig and T.-C. Zheng, *Organometallics*, 1992, **11**, 277; A. Togni, G. Rihs and R. E. Blumber, *Organometallics*, 1992, **11**, 613; C. R. S. M. Hampton, I. R. Butler, W. R. Cullen, B. R. James, J. P. Charland and J. Simpson, *Inorg. Chem.*, 1992, **31**, 5509; M. I. Bruce, P. A. Humphrey, O. Shawkataly, M. R. Snow, E. R. T. Tiekink and W. R. Cullen, *Organometallics*, 1990, **9**, 2910; T. S. A. Hor and L.-T. Phang, *Polyhedron*, 1990, **9**, 2305; T. S. A. Hor, S. P. Neo, C. S. Tan, T. C. W. Mak, K. W. P. Leung and R.-J. Wang, *Inorg. Chem.*, 1992, **31**, 4510; S. T. Chacon, W. R. Cullen, M. I. Bruce, O. Shawkataly, F. W. B. Einstein, R. H. Jones and A. C. Willis, *Can. J. Chem.*, 1990, **68**, 2001; M. Sato and M. Sekino, *J. Organomet. Chem.*, 1993, **444**, 185; J. A. Adeleke and L. K. Liu, *J. Chin. Chem. Soc.*, 1992, **39**, 61; T. Hayashi, A. Yamamoto, Y. Ito, E. Nishioka, H. Miura and K. Yanagi, *J. Am. Chem. Soc.*, 1989, **111**, 6301.

2 K.-S. Gan and T. S. A. Hor, in *Ferrocenes–Homogeneous Catalysis, Organic Synthesis, Materials Science*, eds. A. Togni and T. Hayashi, VCH, Weinheim, 1995, ch. 1, p. 3.

3 U. Casellato, R. Graziani and G. Pilloni, *J. Crystallogr. Spectrosc. Res.*, 1993, **23**, 571.

4 G. Pilloni, R. Graziani, B. Longato and B. Corain, *Inorg. Chim. Acta*, 1991, **190**, 165.

5 S.-P. Neo, T. S. A. Hor, Z.-Y. Zhou and T. C. W. Mak, *J. Organomet. Chem.*, 1994, **464**, 113.

6 L.-T. Phang, T. S. A. Hor, Z.-Y. Zhou and T. C. W. Mak, *J. Organomet. Chem.*, 1994, **469**, 253.

7 T. S. A. Hor, *J. Cluster Sci.*, 1996, **7**, 263, and refs. therein; H. Liu, A. L. C. Tan, C. R. Cheng, K. F. Mok and T. S. A. Hor, *Inorg. Chem.*, 1997, **36**, 2916; H. Liu, A. L. C. Tan, Y. Xu, K. F. Mok and T. S. A. Hor, *Polyhedron*, 1997, **16**, 377; M. Zhou, A. L. C. Tan, Y. Xu, C. F. Lam, P.-H. Leung, K. F. Mok, L.-L. Koh and T. S. A. Hor, *Polyhedron*, 1997, **16**, 2381; A. L. C. Tan, M. L. Chiew and T. S. A. Hor, *J. Mol. Struct.* (*Theochem*), 1997, **393**, 189; H. Liu, A. L. C. Tan, K. F. Mok and T. S. A. Hor, *J. Chem. Soc.*, *Dalton Trans.*, 1996, 4023; M. Zhou, P.-H. Leung, K. F. Mok and T. S. A. Hor, *Polyhedron*, 1996, **15**, 1737.

8 H. Liu, A. L. C. Tan, K. F. Mok, T. C. W. Mak and T. S. A. Hor, *J. Am. Chem. Soc.*, 1997, **119**, 11006; V. W. W. Yam, P. K. Y. Yeung and K. K. Cheung, *Angew. Chem.*, *Int. Ed. Engl.*, 1996, **35**, 739.

9 G. M. Li, S. H. Li, A. L. C. Tan, W.-H. Yip, T. C. W. Mak and T. S. A. Hor, *J. Chem. Soc.*, *Dalton Trans.*, 1996, 4315.

10 P. Braunstein, J.-L. Richert and Y. Dusausoy, *J. Chem. Soc.*, *Dalton Trans.*, 1990, 3801; P. Braunstein, J. Kervennal and J.-L. Richert, *Angew. Chem.*, *Int. Ed. Engl.*, 1985, **24**, 768.

11 H. Bantel, W. Bernhardt, A. K. Powell and H. Vahrenkamp, *Chem. Ber.*, 1988, **121**, 1247; M. C. Grossel, R. P. Moulding and K. R. J. Seddon, *J. Organomet. Chem.*, 1983, **253**, C50.

12 S. Datta and U. C. Agarwala, *Ind. J. Chem.*, *Sect. A*, 1981, **20**, 1190.

13 D. Fenske, in *Clusters and Colloids*, ed. G. Schmid, VCH, Weinheim, 1994; ch. 3.4.3.2, p. 254.

14 H. Werner, W. Bertleff and U. Schubert, *Inorg. Chim. Acta*, 1980, **43**, 199.

15 C. A. Ghilardi, S. Midollini, F. Nuzzi and A. Orlandini, *Transition Met. Chem.*, 1983, **8**, 73.

16 G. Aullon, G. Ujaque, A. Lledos, S. Alvarez and P. Alemany, *Inorg. Chem.*, 1998, **37**, 804.

17 B. Wu, W. J. Zhang, S. Y. Yu, T. L. Sheng and X. T. Wu, *J. Organomet. Chem.*, 1997, **546**, 587.

18 C. E. Briant, T. S. A. Hor, N. D. Howells and D. M. P. Mingos, *J. Chem. Soc.*, *Chem. Commun.*, 1983, 1118.

19 C. K. Johnson, ORTEP, Report ORNL-5138, Oak Ridge National Laboratory, Oak Ridge, TN, 1976.

20 W. Henderson, J. Fawcett, R. D. W. Kemmitt, P. McKenna and D. R. Russell, *Polyhedron*, 1997, **16**, 2455; J. Fawcett, W. Henderson, R. D. W. Kemmitt, D. R. Russell and A. Upreti, *J. Chem. Soc.*, *Dalton Trans.*, 1996, **9**, 1897.

21 (*a*) W. Henderson, A. G. Oliver and A. L. Downard, *Polyhedron*, 1996, **15**, 1165; (*b*) X. Xu, S. P. Nolan and R. B. Cole, *Anal. Chem.*, 1994, **66**, 119.

22 R. Colton, K. L. Harrison, Y. A. Mah and J. C. Traeger, *Inorg. Chim. Acta*, 1995, **231**, 65.

23 T. S. A. Hor, Ph.D. Thesis, University of Oxford, 1983.

24 M. Sato, M. Yamamoto, K. Imada, Y. Katsube, N. Tanaka and T. Higashi, *J. Appl. Crystallogr.*, 1992, **25**, 348; J. Tanner and K. L. Krause, *The Rigaku Journal*, 1992, **11**, 4.

25 T. Higashi, ABSCOR, An Empirical Absorption Correction Based on Fourier Coefficient Fitting, Rigaku Corporation, Tokyo, 1995.

26 G. M. Sheldrick, in *Computational Crystallography*, ed. D. Sayre, Oxford University Press, New York, 1982, p. 506; in *Crystallographic Computing 3: Data Collection, Structure Determination, Proteins and Databases*, eds. G. M. Sheldrick, C. Kruger and R. Goddard, Oxford University Press, New York, 1985, p. 175.

27 G. M. Sheldrick, SHELXL 93, Program for the Refinement of Crystal Structures, University of Göttingen, 1993.

28 L. J. Arnold, *J. Chem. Educ.*, 1992, **69**, 811.

Paper 8/06088F